



## THERMAL AND MECHANICAL PROPERTIES OF ETHYL VINYL ACETATE (EVA) / NANO-CLAYS OR SLAKED LIME COMPOSITES

İlker ERDEM<sup>1\*</sup>, Şeyma AVCI<sup>2</sup>

<sup>1</sup>Abdullah Gül University, Faculty of Engineering, Department of Materials Science and Nanotechnology Engineering, 38080, Kayseri, Türkiye


<sup>2</sup>Abdullah Gül University, Graduate School, Advanced Materials and Nanotechnology MSc Program, 38080, Kayseri, Türkiye


**Abstract:** Ethyl vinyl acetate (EVA) is a widely used copolymer in various industrial applications. One concern about its utilization is its flammability as other polymeric materials. The inorganic fillers like clays, metal hydroxides (e.g. of Al, Mg), metal oxides (e.g. alumina) are evaluated as environmentally benign additives to enhance the flammability characteristics of the polymers. The composites prepared via these inorganic fillers should also be characterized by considering their required mechanical properties for specific applications. The possible utilization of different nano-clays (organically surface modified montmorillonite (MMT)) and “slaked lime” ( $\text{Ca(OH)}_2$  without surface modification) was investigated in the current study. The nano-clay with exfoliated morphology in the EVA matrix was found to be more effective on both mechanical and flammability characteristics of EVA composites.  $\text{Ca(OH)}_2$  was also moderately effective on mechanical and thermal characteristics of the EVA composite. The inorganic filler content of EVA composites may be increased for better flame-retardancy, but the mechanical properties should be investigated simultaneously.

**Keywords:** EVA, Flame-retardancy, Nano-clay, Slaked lime, Mechanical properties

\*Corresponding author: Abdullah Gül University, Faculty of Engineering, Department of Materials Science and Nanotechnology Engineering, 38080, Kayseri, Türkiye

E mail: ilker.erdem@agu.edu.tr (İ. ERDEM)

İlker ERDEM  <https://orcid.org/0000-0001-5743-0835>

Şeyma AVCI  <https://orcid.org/0000-0003-1503-6412>

Received: January 17, 2025

Accepted: March 26, 2025

Published: May 15, 2025

Cite as: Erdem İ, Avcı Ş. 2025. Thermal and mechanical properties of ethyl vinyl acetate (EVA) / nano-clays or slaked lime composites. BSJ Eng Sci, 8(3): 775-783.

### 1. Introduction

Ethyl vinyl acetate (EVA) and its composites have been widely used in various industrial applications (Das et al., 2022; Guo et al., 2018; Jeong et al., 2022; Nyambo et al., 2009; Rafiee and Shahzadi, 2019; Rajczak et al., 2020; Ryu et al., 2020; Tambe et al., 2009). The good compounding properties of the copolymer makes its usage advantageous in different blends (Aghjeh et al., 2015). EVA may have varying acetic acid group (VA) content (10-40 % (Chuayjulit and Worawas, 2011)) which may change its characteristics (e.g. crystallinity, mechanical behavior) (Díez et al., 2021; Luna et al., 2022). Higher VA% decreases the crystallinity of the polymer and increases the polarity of the copolymer, which results in varying characteristics (e.g. blending, mechanical properties) (Chaudhary et al., 2005; Luna et al., 2022). The increasing VA% and increasing polarity may be beneficial for blending of the copolymer with polar additives (e.g. inorganic fillers like clay) which may lead to better interaction and consequently enhanced mechanical properties for EVA/inorganic filler composites (Chaudhary et al., 2005).

The flammability of the polymers is one of the main drawbacks limiting their usage in different applications e.g. where the temperature may rise and creates a risk for ignition (Beyer, 2009; He et al., 2020; Rajczak et al., 2020).

The researchers have been investigating additives to supply flame retardancy to the polymers. The conventional additives which contain halogens are not environmentally friendly and research effort is focused on more environmentally friendly options like inorganic fillers (e.g. oxides, hydroxides, borates) (Dinçer Fil et al., 2025; Dogan et al., 2021; Jeong et al., 2022; Xu et al., 2021). Nano materials with relatively larger surface areas may interact with the surrounding matrix more effectively and that makes their usage advantageous for the preparation of advanced composites. The nano-clay montmorillonite (MMT) is with a layered structure of alternating tetrahedral silicate ( $\text{SiO}_4^{4-}$ ) and octahedral aluminum oxide-hydroxide  $[\text{AlO}_3(\text{OH})_3]_2$  layers with nano thickness. These layers may be separated from each other under appropriate conditions, resulting in platelets with high aspect ratio and nano thickness (i.e. very high surface area). That layer-by-layer separation is called “exfoliation”. The MMT when blended in a polymer matrix (e.g. EVA) may enhance the certain properties of the polymer (e.g. thermal and/or mechanical characteristics). The composites of clay/polymer are used in various industries aerospace, automotive, construction, packaging, water treatment, medical applications, electronics (Das et al., 2022; Guo et al., 2018; Rafiee and Shahzadi, 2019; Tambe et al., 2009).



There are different methods for inorganic filler (e.g. clay)/polymer composite preparation like melt-mixing at high temperature, solvent solution method and sol-gel technique (Das et al., 2022; Guo et al., 2018; Rafiee and Shahzadi, 2019; Ryu et al., 2020). In the solvent solution method, the polymer is dissolved in an appropriate solvent and inorganic filler is dispersed in it. It may result in homogeneously distributed inorganic filler in the composite after drying (evaporation of the solvent). It may assist the exfoliation of the clay, and the polymer may interact with the separate layers of the clay through a larger surface area. The other possible cases for interaction of the polymer and inorganic filler (e.g. clay) are "intercalated" and "agglomerated" morphologies (Figure 1). The polymer may cover the agglomerates of nano-clay (aggregated) or it may penetrate in between the layers of nano-clay (intercalated) or polymer (and solvent) may penetrate and separate the layers of nano-clay and clay platelets may be coated with polymer (exfoliated) (Guo et al., 2018; Rafiee and Shahzadi, 2019). The exfoliated morphology is expected to enhance the interaction of polymer and nano-clay and consequently may present enhanced properties for the composite material.

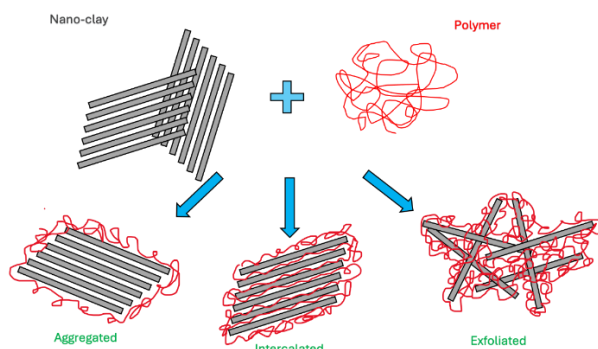


**Figure 1.** Possible morphologies for nano-clay/polymer blends.

Slaked lime ( $\text{Ca(OH)}_2$ ) is a Ca compound taking part in the "lime cycle" (Figure 2). The other forms of Ca in the cycle are "quick lime" ( $\text{CaO}$ ) and "limestone" ( $\text{CaCO}_3$ ). Limestone may be extracted from the Earth's crust in certain regions in considerable quantities. The quick lime ( $\text{CaO}$ ) can be prepared by heating the ground limestone ( $\text{CaCO}_3$ ) at elevated temperatures (e.g. 900-1000 °C). Slaked lime ( $\text{Ca(OH)}_2$ ) can be prepared by soaking the quick lime ( $\text{CaO}$ ) in the water through an exothermic reaction. Like the other hydroxides (e.g., magnesium hydroxide ( $\text{Mg(OH)}_2$ ), aluminum tri hydroxide ( $\text{Al(OH)}_3$ )), slaked lime ( $\text{Ca(OH)}_2$ ) can also serve as an inorganic filler for polymer composites. It may absorb the heat energy during burning of the composite to use it as latent heat to form quick lime ( $\text{CaO}$ ) and water:  $\text{Ca(OH)}_2 + 1/2 \text{O}_2 \rightarrow \text{CaO} + \text{H}_2\text{O}$ . The heat removal decreases the temperature and hampers the burning of the composite. This endothermic reaction for  $\text{Ca(OH)}_2$  takes place at temperatures above 400° C (Oualha et al., 2017). The

water (vapour) produced during the oxidation of the slaked lime ( $\text{Ca(OH)}_2$ ) dilutes the oxygen and flammable thermal degradation of the polymer, which also hampers the burning process. The quick lime ( $\text{CaO}$ ) formed by oxidation may act as a heat/mass transfer resistance which will decrease the transfer of heat and oxygen and/or very flammable low molecular weight (MW) thermal degradation products. These mechanisms may make the slaked lime ( $\text{Ca(OH)}_2$ ) a potential flame-retardant additive for polymer composites. The slaked lime ( $\text{Ca(OH)}_2$ ) is relatively widely produced/used material in industrial applications and it may be supplied easily from different production routes. It is a candidate material for (thermochemical heat) energy storage and/or heat pump applications due to reversible (endo/exo-thermic) dehydration/hydration reaction (Gupta et al., 2021). Zheng et al. (Zheng et al., 2015) reported the energy storage efficiency of  $\text{Ca(OH)}_2$  may be increased by preparing its nanocomposite with Zn. Other possible treatments/methods to enhance energy storage performance of  $\text{Ca(OH)}_2$  were further discussed by Feng et al. (Feng et al., 2023). The slaked lime ( $\text{Ca(OH)}_2$ ), as many other inorganic fillers (e.g. oxides, hydroxides), may affect the mechanical properties of the polymer matrix, too. The possible utilization of the slaked lime ( $\text{Ca(OH)}_2$ ) as a halogen-free flame-retardant additive in polymer composites may be advantageous since it is already available and relatively affordable. Oualha et al. prepared EVA/ $\text{Ca(OH)}_2$  and zinc borate composites with varying ( $\text{Ca(OH)}_2$ ) content (e.g., 20, 40, 60%). They demonstrated the beneficial effect of ( $\text{Ca(OH)}_2$ ) addition on the thermal stability of the EVA/ $\text{Ca(OH)}_2$  composite due to the endothermic effect (Oualha et al., 2017).

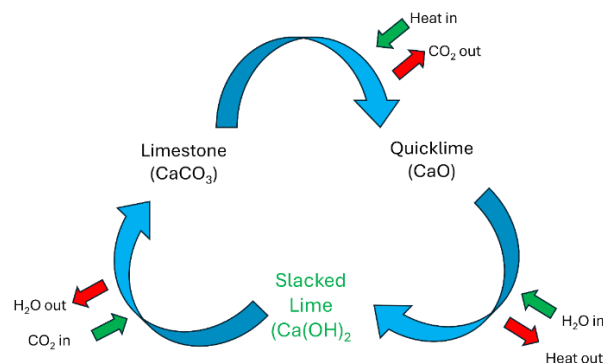


**Figure 2.** The lime cycle.

In this study, the potential of the nano-clays (commercial, with organic surface modifiers for enhanced interaction with polymer) and the slaked lime ( $\text{Ca(OH)}_2$ ) (produced by soaking the quick lime ( $\text{CaO}$ ) in water) as flame-retardant additives for an EVA copolymer was investigated. The effects of both the nano-clays and the slaked lime ( $\text{Ca(OH)}_2$ ) addition on the mechanical properties of the EVA/inorganic filler composites were also estimated to comparatively investigate the potential enhancement/worsening effect of inorganic filler addition in the mechanical durability of the EVA composites. The

results are expected to contribute to the utilization of different inorganic fillers for the preparation of superior EVA composites which have versatile applications.

## 2. Materials and Methods

EVA (with 26 wt. % of VA) was kindly supplied by HES Cable Company (Kayseri, Türkiye). Two different commercial nano-clays from Sigma Co. Ltd. were used. Their surfaces were modified either with 15-35wt.% octadecylamine (Figure 3.a) and 0,5-5 wt.% aminopropyltriethoxysilane (product code 682632) or with 35-45 wt. % dimethyl dialkyl (C14-C18) amine (Figure 3.b) (the product code 682624). The quick lime (CaO) used in the study was from local market and it was "slaked" by soaking it in the tap water overnight. The slaked lime was dried at room temperature and ground before usage. Other chemicals and solvents were products of Merck Co. (Germany).

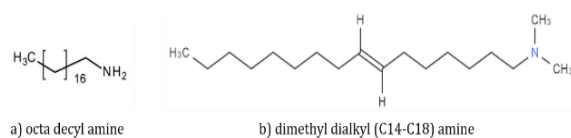


**Figure 3.** Chemical structure of surface modifying compounds for nano-clays

The composites were prepared by solvent solution method. The EVA copolymer (10 phr (parts per hundred)) was dissolved in the organic solvent (chloroform, 100 phr) at elevated temperature (e.g. 40-50 °C) and inorganic fillers (either nano-clay 1 (product code 682632), or nano-clay 2 (the product code 682624), or the slaked lime (10 or 20 phr)) were added gradually. The mixture was kept heated and stirred overnight by using a magnetic stirrer. The mixtures were poured in the glass petri dishes and kept in the hood overnight to evaporate the solvent and prepare the EVA/inorganic filler composites. The samples were named with the abbreviation for the additive and its ratio (phr) e.g. NC-2.20 has 20 phr (parts per hundred) nano-clay 2 in the EVA copolymer. Slaked lime was named as "CaX". The dried composite films were cut to prepare samples for characterization experiments. The strips were cut with a length of 10 to 12.5 cm and a width of 1 to 1.25 cm which were used for tensile test or burning test. The remaining film samples were used for other characterization experiments.

The functional groups of the EVA/inorganic filler composites were analyzed using Fourier transform infrared spectroscopy with an Attenuated Total Reflectance unit (FTIR-ATR, Thermo Scientific Nicolet 6700). The crystallinity of the EVA composites was analyzed via X-Ray Diffraction (XRD) analysis (Bruker D8 Discover, 2 $\theta$ : 0° to 50°, Cu K $\alpha$  radiation ( $\alpha$  = 0.15406 nm)). Thermal analysis of the composites was performed in the temperature range of 30-800 °C (with 10 °C/min heating rate under 20 mL/min nitrogen flow) (Perkin Elmer, STA 8000). The tensile properties of the neat EVA and the

EVA/inorganic filler composites were determined using a Shimadzu AG-X 50kN universal testing instrument according to the ASTM D882 standard ((strain rate: 15 mm  $\times$  s<sup>-1</sup>). Samples prepared considering the UL-94 VTM standard were used for burning test. The time for burning of the sample strips with identical sizes was determined (including the 3 seconds ignition time).

## 3. Results and Discussion

### 3.1. FT-IR Analysis

The chemical bonding/structure of the neat EVA and EVA/inorganic filler composites were analyzed by using FT-IR analysis (Figure 4). The IR spectra of all samples with inorganic fillers are similar to that of the neat EVA copolymer. This indicates no new primary chemical bonding was formed in the composites among the copolymer and the inorganic fillers. The peaks on the IR spectra may be attributed to the EVA copolymer. The peaks observed for the samples were at wavenumber values of 719, 1019, 1237, 1371, 1464, 1733, 2848 and 2916 cm<sup>-1</sup> with slight shifts. The peak at 719 and 1019 cm<sup>-1</sup> were attributed to the C-H rocking and to the C-O stretching vibrations, respectively (Bartolomei et al., 2020). The peaks at 1237 cm<sup>-1</sup> was attributed to vibrations related with C-O bonding (Bartolomei et al., 2020; Ye et al., 2013). The peaks at 1371 and 1464 were reported to be related with -CH<sub>3</sub> symmetric vibration and C-H bending vibrations, respectively (Bartolomei et al., 2020). The peak at 1733 cm<sup>-1</sup> was attributed to the C=O vibration (Luna et al., 2022). The peaks at 2848 and 2916 cm<sup>-1</sup> were attributed to -CH<sub>3</sub> symmetric stretching and C-H asymmetric stretching vibrations, respectively (Bartolomei et al., 2020). The IR absorption was reported for both inorganic fillers at wavenumbers 3620-3740 cm<sup>-1</sup> attributed to the O-H stretching (Zhang et al. 2018; Harish et al., 2022; Akpomie and Dawodu, 2016; Shinde and Shirivastava, 2020), which was not observed in the EVA composites. The possible reason may be the abundance of EVA quantity in comparison to inorganic filler content.

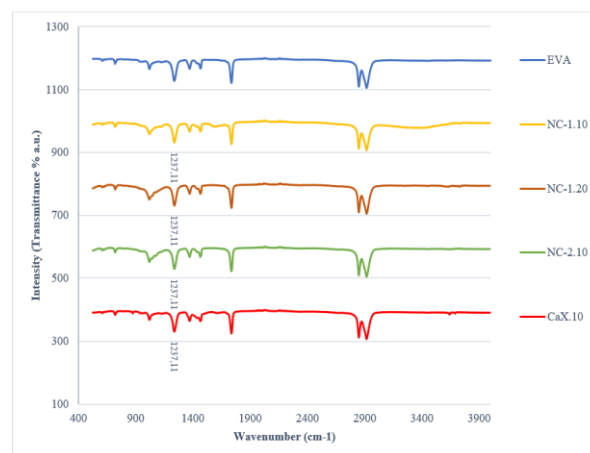


**Figure 4.** FT-IR data (IR spectra of the neat EVA and the EVA/inorganic filler composites.

The results are in accordance with the results by Bartolomei et al. (Bartolomei et al., 2020) who reported that the inorganic fillers didn't make any change in IR spectra of the composites, which was the case in the current study.

### 3.2. X-Ray Diffraction (XRD) Analysis

The X-ray diffractograms of the samples are shown in Figure 5. The characteristic peaks of EVA can be seen for all samples at 2 theta values of 21 and 23°, which are attributed to the planes (110) and (200) (Bartolomei et al., 2020; Díez et al., 2021). The CaX.10 sample has the characteristic peaks for  $\text{Ca}(\text{OH})_2$  (Portlandite, PDF no. 44-1481) at 18°, 28.7° and 34.1° 2 theta values, which are attributed to (001), (100) and (101) planes, respectively. This confirms the formation of "slaked lime" crystals (i.e. the formation of  $\text{Ca}(\text{OH})_2$  using quick lime ( $\text{CaO}$ ) was successful). The nano-clay containing samples were lacking characteristic peaks of clay, only the sample NC-2.10 has a considerable peak at 2 theta value of 6.9° with relatively low intensity, which is indicating the presence of clay crystals which are in agglomerated or intercalated morphology. Peaks at 5.6° and 7.4° 2 theta values were reported for different MMT (montmorillonite) clays (Zhang et al., 2017). There is no considerable peak for NC-1 containing samples showing the nano-clay 1 is totally exfoliated, preventing the scattering of X-rays at certain angle(s).

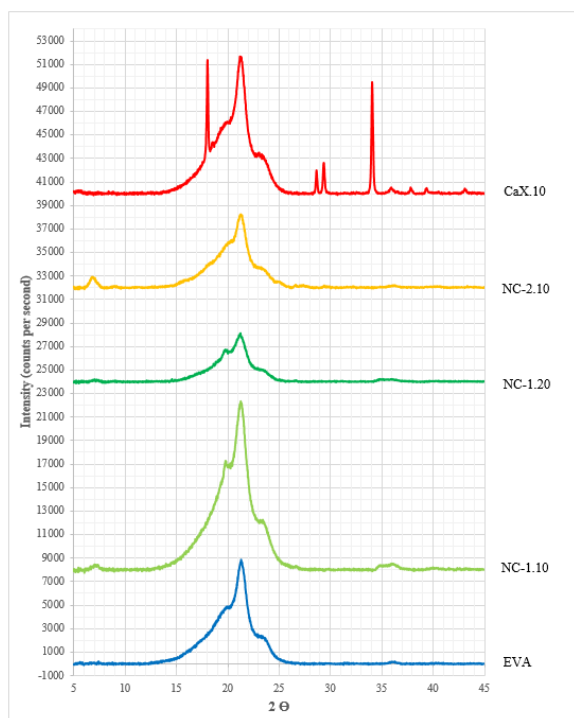


**Figure 5.** XRD diffractograms for the neat EVA (control) and EVA with different inorganic fillers.

### 3.3. Thermogravimetric Analysis (TGA/D-TGA)

The thermal behavior of the samples was characterized via TGA (Figure 6). The onset/off-set temperatures, remaining weight (residue %) at the end of the analysis and the temperatures for certain weight loss percentage

values (5, 10 and 50%) were shown in Table 1 and 2.

The EVA copolymer has two step thermal degradation: i) deacetylation (removal of acetic acid groups), ii) defragmentation (breaking of the main backbone of the polymer chain) (Díez et al., 2021; Luna et al., 2022; Nyambo et al., 2009). The first step was reported to take place at 330-390 °C and second at 430 °C (Luna et al., 2022).

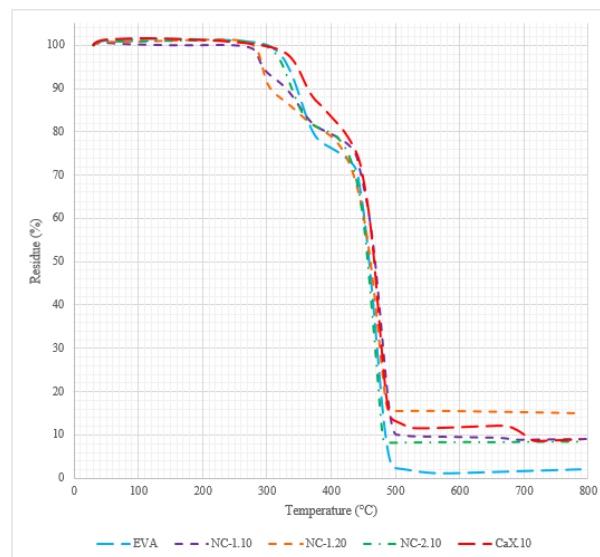


**Figure 6.** TGA data for the neat EVA (control) and the EVA/inorganic filler composites.

The nano-clays (NC-1 and 2) resulted in thermal instability for their EVA composites. The onset temperatures for thermal degradation were lower for the NC1.10 (onset T1: 280 °C) and NC-2.10 (onset T2: 314 °C) than the control (neat EVA) (onset T2: 326 °C), while the composite prepared via  $\text{Ca}(\text{OH})_2$  had a relatively higher onset temperature (onset T2: 341 °C) showing it makes the composite more resistant for thermal degradation initiation. It was reported the presence of  $\text{Ca}(\text{OH})_2$  hampers the deacetylation of EVA composites (the onset temperature was 350 °C for EVA with 20 phr  $\text{Ca}(\text{OH})_2$  which is in accordance with the current results) (Oualha et al., 2017). The lower onset temperature values for the composites with nano-clays may be related to the degradation of the surface modifying organics present in the nano-clays at considerable quantities (15-40 % for NC-1 and 35-45% for NC-2). The neat EVA lost 25% of its weight at this first step of thermal degradation while the composites with inorganic fillers had lower weight loss (%) values (around 20 % for the samples with nano-clays and only 16% for the sample with  $\text{Ca}(\text{OH})_2$ ).

The onset temperatures for the second step of thermal degradation (onset T3) were somehow similar for the neat EVA (449 °C), NC-1.10 (454 °C), NC-1.20 (447 °C) and CaX.10 (450 °C) while it was slightly lower for the sample NC-2.10 (441 °C). The weight loss (%) values for the second step were considerable for all samples; 73.6, 69.5, 65.4, 72.5 and 72.1 % for the samples neat EVA, NC-1.10, NC-1.20, NC-2.10 and CaX.10, respectively.



**Table 1.** The onset/offset temperatures, residue (mass %)

| Sample  | Onset<br>T1 | Δ1<br>(mass%) | Onset<br>T2 | Δ2<br>(mass%) | Onset<br>T3 | Δ3<br>(mass%) | Onset<br>T4 | Δ4<br>(mass%) | Offset<br>T | Residue<br>(mass<br>%) |
|---------|-------------|---------------|-------------|---------------|-------------|---------------|-------------|---------------|-------------|------------------------|
| EVA     | -           | -             | 326.07      | 25.238        | 448.69      | 73.596        | -           | -             | 525.53      | 1.801                  |
| NC-1.10 | 280.29      | 7.465         | 334.75      | 13.159        | 454.41      | 69.538        | -           | -             | 533.24      | 9.669                  |
| NC-1.20 | 280.83      | 13.676        | 359.96      | 7.025         | 448         | 64.994        | -           | -             | 513.10      | 15.547                 |
| NC-2.10 | -           | -             | 314.40      | 20.175        | 441.38      | 72.514        | -           | -             | 494.68      | 8.223                  |
| CaX.10  | -           | -             | 340.59      | 15.825        | 454.75      | 71.184        | 675.12      | 3.483         | 730.98      | 8.665                  |

**Table 2.** The certain weight loss (-5%, -10% and -50%) temperatures

| Sample  | T (-5%) | T (-10%) | T (-50%) |
|---------|---------|----------|----------|
| EVA     | 333.20  | 346.90   | 459.30   |
| NC-1.10 | 293.70  | 329.90   | 468.50   |
| NC-1.20 | 293.10  | 305.60   | 461.30   |
| NC-2.10 | 325.50  | 338.90   | 457.00   |
| CaX.10  | 347.30  | 363.60   | 467.10   |

Unlike the other samples (neat EVA and samples with nano-clays) the sample CaX.10 had another thermal degradation step with onset temperature (onset T4) and weight loss (%) value of 677 °C and 3.5%.

The offset temperature was higher for the control (neat EVA) (526 °C) than the composites NC-1.20 (513 °C), NC-2.10 (495 °C) and lower than NC-1.10 (533 °C) and CaX (731 °C). The remaining weight (residue %) values were 1.8, 9.7, 15.5, 8.2 and 8.6 for the neat EVA, NC-1.10 NC-1.20, NC-2.10 and CaX.10, respectively. These values are in accordance with the added inorganic filler contents. The residue (5) values were higher for the samples with 10 phr inorganic filler addition (NC-2.10 and CaX.10) and it was even higher for the composite with 20 phr inorganic filler (NC-1.20).

The TGA plots for the nano-clay containing samples are sharply becoming constant around 500 °C (Figure 6). But the plots for the sample CaX.10 the plots become constant more slowly which may be attributed to the formation and removal of H<sub>2</sub>O through the reaction:  $(\text{Ca}(\text{OH})_2) + 1/2 \text{O}_2 \rightarrow \text{CaO} + \text{H}_2\text{O}$ , which was reported to take place around 510°C, which requires 148.6 kJ energy (for heating and decomposition) (Zheng et al., 2015) (104.4 kJ/mol (Feng et al., 2023). The defragmentation step of EVA (breaking of the polymer backbone) and dehydroxylation of  $\text{Ca}(\text{OH})_2$  (formation of CaO and water) may happen simultaneously at an overlapping temperature range (400-550 °C) (the second step observed at TGA). This reaction was reported to take place between 375 to 480 °C for the TGA of pure  $\text{Ca}(\text{OH})_2$  (Mirghiasi et al., 2014). The other thermal degradation step observed for the sample CaX.10 at elevated temperatures (onset T4: 677 °C) which may be attributed to the decomposition of  $\text{CaCO}_3$  (calcite) to  $\text{CaO}$ , which was reported to take place between 480 to 650 °C for the TGA of neat  $\text{Ca}(\text{OH})_2$  (Mirghiasi et al., 2014). Oulha et al. reported the onset T as 426 and 525 °C for the decomposition reactions of  $\text{Ca}(\text{OH})_2$  they produced via

eggshell considering the TGA of neat  $\text{Ca}(\text{OH})_2$  (Oualha et al., 2017). They mentioned the possible exothermic contribution of  $\text{Ca}(\text{OH})_2$  at these temperatures hen used as additives in polymer composites (Oualha et al., 2017). The difference in the reaction temperatures for neat  $\text{Ca}(\text{OH})_2$  and its EVA composite (CaX.10) may be due to the presence of polymer (residue) which acts as an extra resistance for heat and mass transfer during TGA. Oulha et al. reported similar TGA results for EVA/ $\text{Ca}(\text{OH})_2$  composites, the offset temperature was above 800 °C for the EVA composite with 20 phr  $\text{Ca}(\text{OH})_2$  (Oualha et al., 2017).

The 5% weight loss was observed at 333, 294, 293, 326 and 347 °C for the neat EVA, NC-1.10, NC-1.20, NC-2.10 and CaX.10, respectively. A similar trend was observed for the T(-10%) values of the samples with the values 347, 330, 306, 339 and 364 °C for the neat EVA, NC-1.10, NC-1.20, NC-2.10 and CaX.10, respectively (Table 2). The 50% weight loss for the samples were observed at 459, 469, 461, 457 and 467 °C for the neat EVA, NC-1.10, NC-1.20, NC-2.10 and CaX.10, respectively. Considering all these temperatures (especially the T(-50%)) sample with 10 phr  $\text{Ca}(\text{OH})_2$  addition (CaX.10) had the highest values which indicates a better thermal stabilization in case of  $\text{Ca}(\text{OH})_2$  utilization (Ryu et al., 2020). NC 1.20 which had double amount of inorganic filler (20 phr nano-clay 2) had similar T(-50%) value with the sample CaX.10.

The derivative-TGA (D-TGA: % weight loss per time) data is shown in Figure 7 and the peak temperature values determined from them are shown in Table 3. There were 2 peak temperatures (peak T2 and T3) values in the same range for all samples. The values for peak T2 were around 351, 352, 343, 337 and 353 °C for the samples neat EVA (control), NC-1.10, NC-1.20, NC-2.10 and CaX.10, respectively (Table 3). The peak temperature decreased for the samples NC-1.20 and NC-2.10 (with surface-modified nano-clays) for this thermal degradation step of

the EVA copolymer, probably due to less thermostable organics used for their surface modifications.

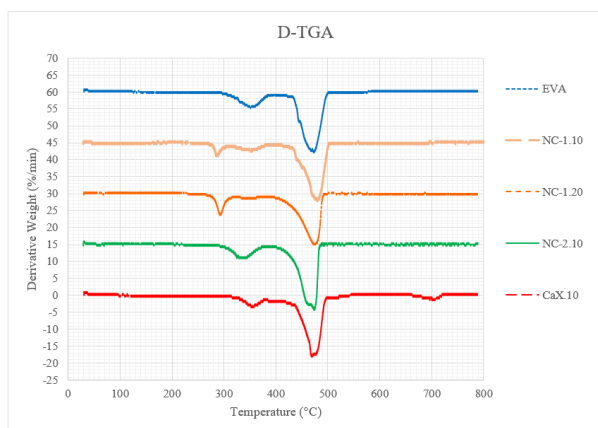


**Figure 7.** D-TGA data for the neat EVA (control) and the EVA/inorganic filler composites.

**Table 3.** The peak temperature values for D-TGA graphs for the control (neat EVA) and the EVA/inorganic filler composites

| Sample  | D-TGA Peak T1 | D-TGA Peak T2 | D-TGA Peak T3 | D-TGA Peak T4 |
|---------|---------------|---------------|---------------|---------------|
| EVA     | -             | 351.19        | 472.26        | -             |
| NC-1.10 | 285.27        | 351.98        | 480.29        | -             |
| NC-1.20 | 291.58        | 342.66        | 476.82        | -             |
| NC-2.10 | -             | 336.59        | 473.92        | -             |
| CaX.10  | -             | 353.36        | 470.37        | 704.63        |

Ca(OH)<sub>2</sub> added 10 phr without any organics slightly increased the peak temperature (peak T2), indicating some enhancement in thermal durability. The peak T3 values were around 472, 480, 477, 474 and 470 °C for the samples neat EVA (control), NC-1.10, NC-1.20, NC-2.10 and CaX.10, respectively (Table 3). For this step of thermal degradation, the nano-clays slightly increased the degradation peak temperature, which may be attributed to the possible extra heat/mass transfer resistance with addition of inorganic filler (nano-clay). The peak T3 value slightly decreased with the addition of Ca(OH)<sub>2</sub> (ΔT was 2 °C), which indicates the Ca(OH)<sub>2</sub> addition didn't enhance the durability at this step of degradation.

There were additional peak temperatures for the samples NC-1.10, NC-1.20 and CaX.10. The sample with 10 or 20 phr nano-clay 1 had a lower degradation peak temperature (peak T1, Table 3), which may be observed due to less thermal durability of the organic surface modifier used in nano-clay 1. Another additional peak temperature was present for the sample with 10 phr Ca(OH)<sub>2</sub> addition (CaX.10) which was around 705 °C (Table 3), which may be attributed to decomposition of calcite.

### 3.4. Tensile Test

The mechanical behavior of the composites and neat EVA was determined via tensile test and the stress-strain

curves are shown in Figure 8. The inorganic fillers increased the stress-bearing capacity of EVA in general. The nano-clays were more effective in increasing the yield strength than the CaX. The type of nano-clay was effective on mechanical characteristics of the composite nano-clay 2 was more effective than nano-clay 1. The sample NC-2.10 (with 10 phr nano-clay 2) could bear higher stress than the samples NC-1.10 and NC-1.20 (with 20 phr nano-clay 2). The increasing amount of nano-clay didn't affect the stress bearing capacity considerably but increased the elongation (%) at break. CaX addition increased the stress bearing capacity slightly. The stress-strain curve of the sample CaX.10 was different than the other samples. At higher strain values the stress increased with a higher slope indicating the CaX showed a higher resistance in elongation at similar strain levels before fracture (which occurred at a relatively lower strain value than the other samples indicating a more brittle (i.e. less ductile) characteristic. The higher stress bearing capacity of the sample NC-2.10 can be attributed to its exfoliated morphology which increased the interaction between the organically surface modified nano-clay and the polymer matrix. CaX without any surface modification not that much effective as surface modified nano-clays up to certain stress values, but after certain strain values it was more resistive.

The Young's modulus values for the neat EVA (control) and composites with inorganic fillers are shown in Figure 9. The CaX addition increased the modulus 21%, while nano-clay addition increased more considerably. The modulus increased 71, 220, and 139% for the samples NC-1.10, NC-1.20 and NC-2.10, respectively. The nano-clay type and ratio were both effective in increasing the Young's modulus value of the EVA composite. More exfoliated nano-clay 2 resulted in a higher modulus value than both nano-clay 1 and CaX at similar ratio (10 phr). Increasing the organically surface-modified inorganic filler from 10 phr to 20 phr resulted in an 87% higher modulus.

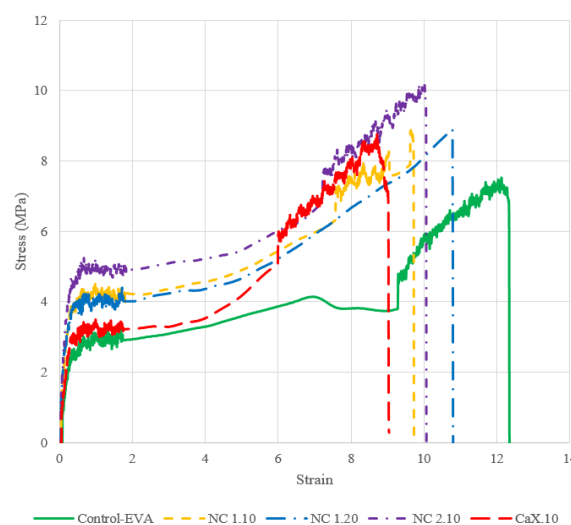


**Figure 8.** Tension test data for the neat EVA (control) and the composites.

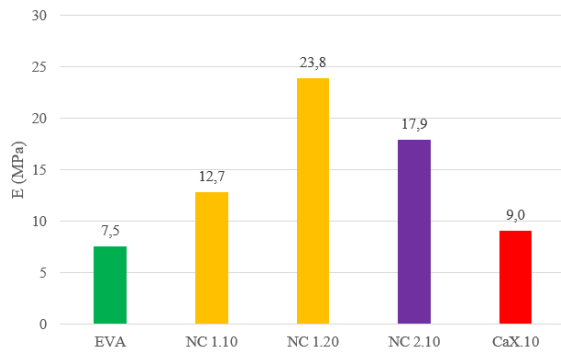


**Figure 9.** Young's Modulus values for the neat EVA (control) and the composites.

### 3.4. Burning Test

The neat EVA and its composites with inorganic fillers were burned considering the UL-94 VTM standard test. The samples were found to be non-self-extinguishing and there were drippings during burning (i.e. the samples failed the test). The burning times for total burning were recorded to compare the hampering effects of different inorganic fillers (Figure 10). The inorganic fillers increased the time for complete burning. The increase was 25% for CaX.10 and 38% for NC-2.10, while it was higher for samples with nano-clay 1 (64% and 105% for NC-1.10 and NC-1.20, respectively). Samples with nano-clay 1 with exfoliated morphology (i.e. well suspended platelets in the polymer matrix) resulted in a more efficient resistance for mass and heat transfer in the composite which increased the time for complete burning. The intercalated nano-clay 2 and CaX in the EVA composite also increased the burning time but less than the totally exfoliated nano-clay 1, showing the importance of distribution of inorganic filler in the polymer matrix. The inorganic filler content can be increased, and different fillers may be added simultaneously for possible enhancement in flame retardancy.

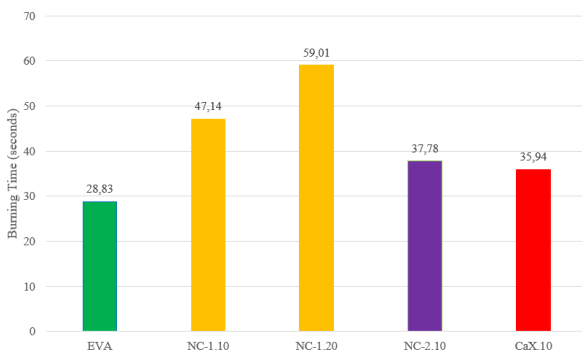


**Figure 10.** Burning time values for the neat EVA (control) and the composites.

## 4. Conclusion

EVA is one of the most widely used polymers in various industries. But its flammability is a drawback for applications where high temperatures or ignition risks are present. The inorganic fillers may be used to enhance the flammability characteristics of EVA composites, but the

effect of inorganic filler addition on mechanical characteristics of the composite should also be considered. In this study organically surface-modified nano-clays and slaked lime ( $\text{Ca}(\text{OH})_2$ ) were used to prepare EVA composites and the change in thermal durability and mechanical characteristics were investigated.

The nano-clay type and ratio were effective on both mechanical and thermal characteristics of the EVA composites. NC-2.10 had the highest load-bearing capacity which has an intercalated morphology. It has the highest Young's modulus value among the samples with similar inorganic filler content (10 phr). The highest burning time was of the samples NC-1.10 and NC-1.20 (with 10 phr and 20 phr of nano-clay 1). The totally exfoliated morphology may be effective on having a more homogeneous structure in the composite and better resistance against mass and heat transfer resulting in longer burning times.  $\text{Ca}(\text{OH})_2$  was moderately effective on mechanical and thermal characteristics of the EVA composite. It slightly increased the Young's modulus (21%) and burning time (25%). The sample with  $\text{Ca}(\text{OH})_2$  (CaX.10) was with less ductility among all samples and its stress-bearing characteristics was different than the other samples. Possible contribution of surface modification for the slaked lime on its interaction with the polymer matrix may be investigated.

The incorporation of inorganic fillers into EVA copolymer increased the burning times of the resultant composites, but the samples did not exhibit self-extinguishing behavior. The filler content can be increased, and they may be used simultaneously for better flame-retardancy properties. The mechanical properties are considerably changing with the inorganic filler type and ratio. Therefore, the mechanical characterization should be performed for changing composite recipes, as well, to satisfy the criteria for specific applications.

### Author Contributions

The percentages of the authors' contributions are presented below. All authors reviewed and approved the final version of the manuscript.

|     | İ.E. | Ş.A. |
|-----|------|------|
| C   | 100  | 0    |
| D   | 100  | 0    |
| S   | 100  | 0    |
| DCP | 50   | 50   |
| DAI | 50   | 50   |
| L   | 60   | 40   |
| W   | 60   | 40   |
| CR  | 60   | 40   |
| SR  | 90   | 10   |
| PM  | 100  | 0    |
| FA  | 100  | 0    |

C=Concept, D= design, S= supervision, DCP= data collection and/or processing, DAI= data analysis and/or interpretation, L= literature search, W= writing, CR= critical review, SR= submission and revision, PM= project management, FA= funding acquisition.

### Conflict of Interest

The authors declared that there is no conflict of interest.

### Ethical Consideration

Ethics committee approval was not required for this study because there was no study on animals or humans.

### Acknowledgements

Ethyl vinyl acetate (EVA) copolymer was kindly supplied by HES KABLO (Kayseri, TR).

### References

- Aghjeh MR, Nazari M, Khonakdar HA, Jafari SH, Wagenknecht U, Heinrich G. 2015. In depth analysis of micro-mechanism of mechanical property alternations in PLA/EVA/clay nanocomposites: A combined theoretical and experimental approach. *Mater Des*, 88: 1277-1289.
- Akpomei KG, Dawodu FA. 2016. Acid-modified montmorillonite for sorption of heavy metals from automobile effluent. *Beni-Suef Uni J Basic App Sci*, 5: 1-12.
- Bartolomei SS, Santana JG, Valenzuela Díaz FR, Kavaklı PA, Guven O, Moura EAB. 2020. Investigation of the effect of titanium dioxide and clay grafted with glycidyl methacrylate by gamma radiation on the properties of EVA flexible films. *Radiat Phys Chem*, 169: 107973.
- Beyer G. 2009. Nanocomposites - a new class of flame retardants. *Plastics Addit Compounding*, 11(2): 16-21.
- Chaudhary DS, Prasad R, Gupta RK, Bhattacharya SN. 2005. Clay intercalation and influence on crystallinity of EVA-based clay nanocomposites. *Thermochim Acta*, 433(1-2): 187-195.
- Chuayjuljit S, Worawas C. 2011. Nanocomposites of EVA/polystyrene nanoparticles/montmorillonite. *J Compos Mater*, 45(6): 631-638.
- Das P, Manna S, Behera AK, Shee M, Basak P, Sharma AK. 2022. Current synthesis and characterization techniques for clay-based polymer nano-composites and its biomedical

- applications: A review. *Environ Res*, 212: 113534.
- Díez E, Rodríguez A, Gómez JM, Galán J. 2021. TG and DSC as tools to analyse the thermal behaviour of EVA copolymers. *J Elastomers Plast*, 53(7): 792-805.
- Dinçer Fil S, Alp FB, Gönen M. 2025. Techno-economic analysis of zinc borate production from zinc oxide and boric acid. *J Black Sea Eng Sci*, 8(1): 119-127.
- Dogan M, Dogan SD, Savas LA, Ozelik G, Tayfun U. 2021. Flame retardant effect of boron compounds in polymeric materials. *Compos B Eng*, 222: 109088.
- Feng Y, Li X, Wu H, Li C, Zhang M, Yang H. 2023. Critical review of Ca(OH)<sub>2</sub>/CaO thermochemical energy storage materials. *Energies Basel*, 16(7): 3019.
- Guo F, Aryana S, Han Y, Jiao Y. 2018. A review of the synthesis and applications of polymer-nanoclay composites. *Appl Sci Basel*, 8(9): 1696.
- Gupta A, Armatas PD, Sabharwall P, Fronk BM, Utgikar V. 2021. Thermodynamics of Ca(OH)<sub>2</sub>/CaO reversible reaction: Refinement of reaction equilibrium and implications for operation of chemical heat pump. *Chem Eng Sci*, 230: 116227.
- Harish Kumar P, Soni A, Chakinala AG, Singhal R, Joshi RP, Mukhopadhyay AK. 2022. Effect of molarity on methylene blue dye removal efficacy of nano Ca(OH)<sub>2</sub>. *ChemistrySelect*, 7: e202200393.
- He W, Song P, Yu B, Fang Z, Wang H. 2020. Flame retardant polymeric nanocomposites through the combination of nanomaterials and conventional flame retardants. *Prog Mater Sci*, 114: 100687.
- Jeong SH, Park CH, Song H, Heo JH, Lee JH. 2022. Biomolecules as green flame retardants: Recent progress, challenges, and opportunities. *J Clean Prod*, 368: 133241.
- Luna CBB, da Silva Barbosa Ferreira E, Siqueira DD, dos Santos Filho EA, Araújo EM. 2022. Additivation of the ethylene-vinyl acetate copolymer (EVA) with maleic anhydride (MA) and dicumyl peroxide (DCP): the impact of styrene monomer on cross-linking and functionalization. *Polym Bull*, 79(9): 7323-7346.
- Mirghiasi Z, Bakhtiari F, Darezereshki E, Esmaeilzadeh E. 2014. Preparation and characterization of CaO nanoparticles from Ca(OH)<sub>2</sub> by direct thermal decomposition method. *J Ind Eng Chem*, 20(1): 113-117.
- Nyambo C, Kandare E, Wilkie CA. 2009. Thermal stability and flammability characteristics of ethylene vinyl acetate (EVA) composites blended with a phenyl phosphonate-intercalated layered double hydroxide (LDH), melamine polyphosphate and/or boric acid. *Polym Degrad Stab*, 94(4): 513-520.
- Oualha MA, Amdouni N, Laoutid F. 2017. Synergistic flame-retardant effect between calcium hydroxide and zinc borate in ethylene-vinyl acetate copolymer (EVA). *Polym Degrad Stab*, 144: 315-324.
- Rafiee R, Shahzadi R. 2019. Mechanical properties of nanoclay and nanoclay reinforced polymers: A review. *Polym Compos*, 40(2): 431-445.
- Rajczak E, Arrigo R, Malucelli G. 2020. Thermal stability and flame retardance of EVA containing DNA-modified clays. *Thermochim Acta*, 686: 178546.
- Ryu HJ, Hang NT, Lee JH, Choi JY, Choi G, Choy JH. 2020. Effect of organo-smectite clays on the mechanical properties and thermal stability of EVA nanocomposites. *Appl Clay Sci*, 196: 105750.
- Shinde SG, Shrivastava VS. 2020. Ni and Zn modified acid activated montmorillonite clay for effective removal of carbol fuchsin dye from aqueous solution. *SN Appl Sci*, 2: 519.
- Tambe SP, Naik RS, Singh SK, Patri M, Kumar D. 2009. Studies on effect of nanoclay on the properties of thermally sprayable



- EVA and EVAI coatings. *Prog Org Coat*, 65(4): 484-489.
- Xu YJ, Qu LY, Liu Y, Zhu P. 2021. An overview of alginates as flame-retardant materials: Pyrolysis behaviors, flame retardancy, and applications. *Carbohydr Polym*, 260: 117827.
- Ye L, Miao Y, Yan H, Li Z, Zhou Y, Liu J, Liu H. 2013. The synergistic effects of boroxo siloxanes with magnesium hydroxide in halogen-free flame retardant EVA/MH blends. *Polym Degrad Stab*, 98(4): 868-874.
- Zhang H, Wang W, Li L, Liu J. 2018. Starch-assisted synthesis and characterization of layered calcium hydroxide particles. *J Inorg Organometal Poly Mat*, 28: 2399-2406.
- Zhang X, Yi H, Bai H, Zhao Y, Min F, Song S. 2017. Correlation of montmorillonite exfoliation with interlayer cations in the preparation of two-dimensional nanosheets. *RSC Adv*, 7(66): 41471-41478.
- Zheng M, Sun SM, Hu J, Zhao Y, Yu LJ. 2015. Preparation of nano-composite  $\text{Ca}_2\text{-}\alpha\text{Zn}\alpha(\text{OH})_4$  with high thermal storage capacity and improved recovery of stored heat energy. *Open Eng*, 5(1): 42-47.